J. Fluid Mech. (1987), *vol.* 183, *pp.* 199–218
Printed in Great Britain

The lift force on a spherical body in a rotational flow

By T. R. AUTON†

Department of Applied Mathematics and Theoretical Physics, University of Cambridge, Silver Street, Cambridge CB3 9EW, UK

(Received 21 December 1981 and in revised form 31 December 1986)

This paper concerns the flow about a sphere placed in a weak shear flow of an inviscid fluid. The secondary velocity resulting from advection of vorticity by the irrotational component of the flow is computed on the sphere surface, and on the upstream axis. The resulting lift force on the sphere is evaluated, and the result is confirmed by an analytical far-field calculation. The displacement of the stagnation streamline, far upstream of the sphere, is calculated more accurately than in previous papers.

1. Introduction

The magnitude of forces acting on small bubbles, droplets and particles in non-uniform and unsteady flows is still a subject of some controversy, even when the flow is inviscid and the shapes are spherical. The force on a stationary or moving sphere in a uniform unsteady flow is well known (e.g. Batchelor 1967). The force on a sphere in a non-uniform irrotational flow was first derived by Taylor (1928) and Tollmien (1938), and subsequently re-derived by a number of authors (see Auton, Hunt & Prud'homme 1987); but there has been no published calculation of the force on a sphere in an inviscid rotational flow.

As well as being of fundamental interest for many problems in fluid mechanics, there are practical applications of knowledge of the forces on a sphere in inviscid flow. The chief one is in calculating the motion of bubbles in pure water when the Reynolds number is large, the wake is thin and the outer flow is close to that calculated in inviscid flow. Calculating the force on bubbles in rotational flow could lead to a better understanding of the distribution of bubbles in pipe flow and in vortices, situations of importance but whose analysis remains quite uncertain.

Whereas the analysis of irrotational flow around a sphere is linear, that of rotational flow is, in general, nonlinear. However the latter analysis is approximately linear if the strength of the vorticity of the rotational flow is weak enough that the change in incident velocity across the sphere ($|\omega| a$) is much less than the relative difference between the velocity of the sphere $\boldsymbol{U}$ and the incident velocity $\boldsymbol{u}_0$ on the centre of the sphere, i.e.

$$|\omega| a \ll |\boldsymbol{U}-\boldsymbol{u}_0|. \tag{1.1}$$

Given the approximation (1.1), Lighthill (1956*a*, *b*) showed how the velocity field can be calculated to a first approximation by calculating how the vorticity of the weak rotational velocity field is distributed by the primary, irrotational velocity field proportional to $|\boldsymbol{U}-\boldsymbol{u}_0|$. Once the distorted vorticity is calculated, the secondary flow

† Present address: Imperial Chemical Industries PLC, Central Toxicology Laboratory, Alderley Park, Macclesfield, Cheshire SK10 4TJ, UK.

associated with these changes can be computed by the Biot–Savart law, and using the method of images to satisfy the appropriate boundary conditions on the sphere.

In this paper Lighthill's technique is followed in detail to compute the velocity field, the surface pressure and thence the force acting on the sphere. It is shown that certain arithmetic (or typographic) errors were made by Lighthill (1957) and Cousins (1969, 1970) in their calculations of the velocity and pressure fields. Neither author calculated the complete pressure field or the net force acting on the sphere. Analysis shows that this must be a lift force equal to

$$\boldsymbol{F}_L = C_L \tfrac{4}{3}\pi a^3 \rho^* (\boldsymbol{U} - \boldsymbol{u}_0) \wedge \boldsymbol{\omega}, \tag{1.2}$$

where ρ^* is the fluid density and C_L the lift coefficient.

Computations of C_L gives a value of 0.500, and a subsequent control volume analysis given in §6 confirms that $C_L = \frac{1}{2}$.

This result is used in a more general analysis of spherical particles in non-uniform flows by Auton *et al.* (1987).

2. Statement of the problem

A slightly sheared plane parallel flow approaches a fixed sphere of radius a. The problem is to calculate the velocity field $\boldsymbol{u}(\boldsymbol{x})$ around the sphere, the pressure distribution on the sphere p, and the lift force $\boldsymbol{F}_L$ acting on the sphere, subject to the assumptions that the viscosity is zero, the density is uniform and the shear is weak but uniform. Formally a solution is to be found to the governing equations

$$(\boldsymbol{u} \cdot \nabla)\boldsymbol{\omega} = (\boldsymbol{\omega} \cdot \nabla)\boldsymbol{u}, \tag{2.1}$$

where

$$\boldsymbol{\omega} = \nabla \wedge \boldsymbol{u} \tag{2.2}$$

and

$$\nabla \cdot \boldsymbol{u} = 0, \tag{2.3}$$

subject to the boundary conditions

$$\boldsymbol{u} = (u_0 + Ay, 0, 0)^{\mathrm{T}} \quad \text{as } x \to -\infty \tag{2.4}$$

and

$$\boldsymbol{u} \cdot \boldsymbol{n} = 0 \quad \text{on } r = a; \tag{2.5}$$

$\boldsymbol{u}_0$ and A are constants. We seek an approximate solution when

$$\tilde{A} = \frac{aA}{u_0} \ll 1 \tag{2.6}$$

(which is the first term in an asymptotic expansion as $\tilde{A} \to 0$).

The solution is based upon that of Lighthill (1956*a*, *b*, 1957). $\boldsymbol{u}$ is the sum of the irrotational (or primary) flow $\boldsymbol{V}$ past a sphere (i.e. $\tilde{A} = 0$) plus a small perturbation (or secondary) velocity field $\boldsymbol{v}$, proportional to $\tilde{A}u_0$, i.e.

$$\boldsymbol{u} = \boldsymbol{V} + \boldsymbol{v}, \tag{2.7}$$

where

$$\nabla \wedge \boldsymbol{V} = 0$$

and

$$\boldsymbol{V} \to (u_0, 0, 0)^{\mathrm{T}} \quad \text{as } r \to \infty \tag{2.8}$$

$$\boldsymbol{V} \cdot \boldsymbol{n} = 0 \quad \text{on } r = a.$$

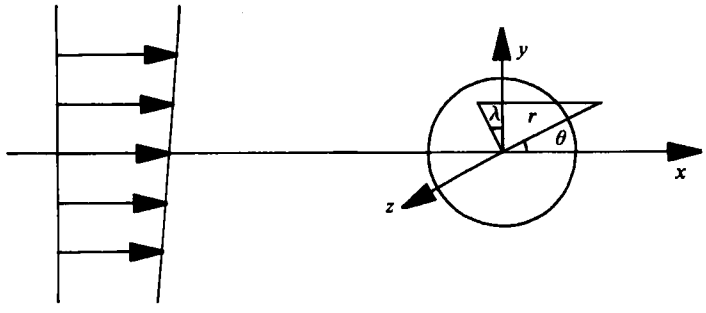

FIGURE 1. The configuration of the Cartesian and spherical polar coordinates.

Therefore, in terms of spherical polar coordinates (r, θ, λ) as shown on figure 1, the solution to $\boldsymbol{V}$ is

$$\left.\begin{aligned} V_r &= u_0\left(1-\frac{a^3}{r^3}\right)\cos\theta, \\ V_\theta &= -u_0\left(1+\frac{1}{2}\frac{a^3}{r^3}\right)\sin\theta, \\ V_\lambda &= 0. \end{aligned}\right\} \tag{2.9}$$

The primary-flow streamlines are defined by

$$r^2\sin^2\theta\left(1-\frac{a^3}{r^3}\right) = \rho_0^2, \tag{2.10}$$

where ρ_0 is the distance of the streamline from the axis far upstream of the sphere.

From (2.1), (2.6) and (2.8) it follows that to first order $\boldsymbol{v}$ satisfies

$$(\boldsymbol{V}\cdot\boldsymbol{\nabla})\,\boldsymbol{\omega} = (\boldsymbol{\omega}\cdot\boldsymbol{\nabla})\,\boldsymbol{V} \tag{2.11}$$

where $$\boldsymbol{\omega} = \boldsymbol{\nabla}\wedge\boldsymbol{v}$$

and $$\boldsymbol{\omega}\to(0, 0, -A)^{\mathrm{T}} \quad \text{as } x\to-\infty, \tag{2.12}$$

where the second-order terms $(\boldsymbol{v}\cdot\boldsymbol{\nabla})\,\boldsymbol{\omega}$ and $(\boldsymbol{\omega}\cdot\boldsymbol{\nabla})\,\boldsymbol{v}$ of $O(\tilde{A}^2)$ can be neglected when $\tilde{A} \ll 1$. (This approximation is not uniformly valid; it is not valid in particular near to the stagnation points of the primary flow.) The solution to (2.11) for the vorticity of the secondary flow, subject to (2.12) is defined by the primary velocity field. Lighthill (1956*b*) showed how this solution for $\boldsymbol{\omega}$ can be expressed in terms of the drift function t defined by

$$\mathrm{d}t = \frac{\mathrm{d}x}{V_x} = \frac{\mathrm{d}y}{V_y} = \frac{\mathrm{d}z}{V_z}, \tag{2.13}$$

$$t - \frac{x}{u_0} \to 0 \quad \text{as } x\to-\infty. \tag{2.14}$$

Notice that the surfaces of constant t describe the motion of planes initially perpendicular to the flow far upstream when convected by the primary flow. Cousins (1969) gives the following expression for t, which is convenient for numerical integration as it removes the singularity in the integrand when $\theta\to\pi$:

$$u_0\,t(\rho_0, \theta) = \int_\theta^\pi \left(\frac{r'}{(1+\frac{1}{2}(a^3/r'^3))\sin\theta'} - \frac{\rho_0}{\sin^2\theta'}\right)\mathrm{d}\theta' + \rho_0\cot\theta, \tag{2.15}$$

θ	$\rho/a = 0.1000$	0.2500	0.5000	1.0000	2.0000
0.00	−13.0203	−4.7568	−1.8393	−0.4006	−0.0240
10.00	−3.3288	−3.5797	−1.7331	−0.3916	−0.0235
20.00	−0.6889	−1.5231	−1.2732	−0.3493	−0.0208
30.00	0.0209	−0.5039	−0.6988	−0.2578	−0.0129
40.00	0.3650	0.0239	−0.2362	−0.1257	0.0025
50.00	0.5828	0.3437	0.0992	0.0203	0.0249
60.00	0.7345	0.5555	0.3380	0.1556	0.0511
70.00	0.8393	0.6980	0.5040	0.2648	0.0759
80.00	0.9045	0.7880	0.6114	0.3402	0.0941
90.00	0.9333	0.8334	0.6687	0.3787	0.1018
100.00	0.9277	0.8390	0.6812	0.3805	0.0978
110.00	0.8893	0.8079	0.6527	0.3481	0.0834
120.00	0.8205	0.7431	0.5865	0.2869	0.0623
130.00	0.7238	0.6474	0.4860	0.2066	0.0396
140.00	0.6025	0.5235	0.3564	0.1220	0.0203
150.00	0.4602	0.3740	0.2089	0.0525	0.0076
160.00	0.2999	0.2022	0.0744	0.0129	0.0017
170.00	0.1216	0.0390	0.0068	0.0009	0.0001
180.00	0	0	0	0	0

TABLE 1. $\omega_{1r}/A \sin\lambda$

where r' is the positive root of

$$r'^2\left(1-\frac{a^3}{r'^3}\right) = \rho_0^2 \operatorname{cosec}^2\theta'. \tag{2.16}$$

The vorticity is then given in terms of t by (Lighthill 1956*b*, equation (58))

$$\left.\begin{aligned} \omega_r &= A\sin\lambda\left(V_r\left(\frac{\partial t}{\partial\rho_0}\right)_\theta - \left(\frac{\partial r}{\partial\rho_0}\right)_\theta\right), \\ \omega_\theta &= A\sin\lambda\left(V_\theta\left(\frac{\partial t}{\partial\rho_0}\right)_\theta\right), \\ \omega_\lambda &= -A\cos\lambda\frac{r\sin\theta}{\rho_0}. \end{aligned}\right\} \tag{2.17}$$

Notice the very simple form of ω_λ. The ring vorticity is independent of t, as the axisymmetric primary flow causes stretching, but not rotation, of ring vorticity.

It is convenient to subtract from ω the uniform oncoming vorticity field. So we define

$$\omega_1 = \omega - \omega_0, \tag{2.18}$$

where

$$\left.\begin{aligned} \omega_{0r} &= -A\sin\lambda\sin\theta, \\ \omega_{0\theta} &= -A\sin\theta\cos\theta, \\ \omega_{0\lambda} &= -A\cos\lambda. \end{aligned}\right\} \tag{2.19}$$

Numerically calculated values of ω_1 and r/a as functions of ρ_0/a and θ are given in tables 1–4. The values of ω_1, agree with those given by Lighthill (1956*b*) to within 0.1. Lighthill's results are not as accurate as those given here, as he used an asymptotic approximation to calculate t, rather than a numerical integration of (2.15).

θ	$\rho/a = 0.1000$	0.2500	0.5000	1.0000	2.0000
0	0	0	0	0	0
10.00	2.1611	0.7837	0.3057	0.0672	0.0039
20.00	3.9730	1.5256	0.5716	0.1213	0.0059
30.00	5.5280	2.1547	0.8122	0.1601	0.0054
40.00	6.8714	2.6622	1.0150	0.1889	0.0031
50.00	7.9870	3.0562	1.1693	0.2121	0.0008
60.00	8.8498	3.3377	1.2724	0.2305	0.0003
70.00	9.4376	3.5052	1.3243	0.2427	0.0024
80.00	9.7345	3.5578	1.3266	0.2474	0.0069
90.00	9.7329	3.4963	1.2815	0.2434	0.0127
100.00	9.4336	3.3244	1.1924	0.2302	0.0180
110.00	8.8463	3.0487	1.0639	0.2077	0.0212
120.00	7.9896	2.6791	0.9018	0.1762	0.0213
130.00	6.8902	2.2288	0.7137	0.1372	0.0181
140.00	5.5829	1.7146	0.5099	0.0934	0.0126
150.00	4.1105	1.1595	0.3053	0.0508	0.0067
160.00	2.5269	0.6009	0.1268	0.0183	0.0023
170.00	0.9261	0.1363	0.0200	0.0026	0.0003
180.00	0	0	0	0	0

TABLE 2. $\omega_{1\theta}/A \sin\lambda$

θ	$\rho/a = 0.1000$	0.2500	0.5000	1.0000	2.0000
0	0	0	0	0	0
10.00	−0.9277	−0.1378	−0.0203	−0.0026	−0.0003
20.00	−2.5176	−0.6096	−0.1325	−0.0194	−0.0025
30.00	−4.0667	−1.1663	−0.3247	−0.0575	−0.0077
40.00	−5.4797	−1.7007	−0.5420	−0.1129	−0.0162
50.00	−6.7040	−2.1729	−0.7484	−0.1757	−0.0270
60.00	−7.6987	−2.5603	−0.9238	−0.2352	−0.0384
70.00	−8.4324	−2.8474	−1.0563	−0.2832	−0.0483
80.00	−8.8819	−3.0238	−1.1385	−0.3141	−0.0551
90.00	−9.0333	−3.0833	−1.1663	−0.3247	−0.0575
100.00	−8.8819	−3.0238	−1.1385	−0.3141	−0.0551
110.00	−8.4324	−2.8474	−1.0563	−0.2832	−0.0483
120.00	−7.6987	−2.5603	−0.9238	−0.2352	−0.0384
130.00	−6.7040	−2.1729	−0.7484	−0.1757	−0.0270
140.00	−5.4797	−1.7007	−0.5420	−0.1129	−0.0162
150.00	−4.0667	−1.1663	−0.3247	−0.0575	−0.0077
160.00	−2.5176	−0.6096	−0.1325	−0.0194	−0.0025
170.00	−0.9277	−0.1378	−0.0203	−0.0026	−0.0003
180.00	0	0	0	0	0

TABLE 3. $\omega_{1\lambda}/A \cos\lambda$

3. The secondary velocity field

The secondary velocity field $\boldsymbol{v}$ consists of four parts:

$\boldsymbol{v}_0^{\mathrm{e}}$, the uniform shear-flow perturbation;

$\boldsymbol{v}_0^{\mathrm{i}}$, an irrotational flow field such that $\boldsymbol{v}_0 \cdot \boldsymbol{n} = (\boldsymbol{v}_0^{\mathrm{e}} + \boldsymbol{v}_0^{\mathrm{i}}) \cdot \boldsymbol{n} = 0$ on the surface of the sphere;

$\boldsymbol{v}_1^{\mathrm{e}}$, the Biot–Savart velocity field due to the vorticity $\boldsymbol{\omega}_1$;

θ	$\rho/a = 0.1000$	0.2500	0.5000	1.0000	2.0000
10.00	1.1101	1.6380	2.9379	5.7738	11.5213
20.00	1.0285	1.1765	1.6556	2.9806	5.8622
30.00	1.0133	1.0832	1.3247	2.1149	4.0309
40.00	1.0081	1.0504	1.1995	1.7314	3.1619
50.00	1.0057	1.0355	1.1412	1.5348	2.6813
60.00	1.0044	1.0278	1.1107	1.4263	2.3980
70.00	1.0038	1.0236	1.0941	1.3656	2.2312
80.00	1.0034	1.0215	1.0857	1.3344	2.1427
90.00	1.0033	1.0208	1.0832	1.3247	2.1149
100.00	1.0034	1.0215	1.0857	1.3344	2.1427
110.00	1.0038	1.0236	1.0941	1.3656	2.2312
120.00	1.0044	1.0278	1.1107	1.4263	2.3980
130.00	1.0057	1.0355	1.4112	1.5348	2.6813
140.00	1.0081	1.0504	1.1995	1.7314	3.1619
150.00	1.0133	1.0832	1.3247	2.1149	4.0309
160.00	1.0285	1.1765	1.6556	2.9806	5.8622
170.00	1.1101	1.6380	2.9379	5.7738	11.5213

TABLE 4. r/a

$\boldsymbol{v}_1^{\mathrm{i}}$, an irrotational flow field such that $\boldsymbol{v}_1 \cdot \boldsymbol{n} = (\boldsymbol{v}_1^{\mathrm{e}} + \boldsymbol{v}_1^{\mathrm{i}}) \cdot \boldsymbol{n} = 0$ on the surface of the sphere.

$\boldsymbol{v}_0^{\mathrm{e}}$ and $\boldsymbol{v}_0^{\mathrm{i}}$ are easily determined. $\boldsymbol{v}_0^{\mathrm{i}}$ has velocity potential

$$\phi_0^{\mathrm{i}} = \frac{Aa^5}{3r^3} \sin\theta \cos\theta \cos\lambda \tag{3.1}$$

and $\boldsymbol{v}_0$ is given by

$$\left.\begin{aligned} v_{0r} &= Ar \sin\theta \cos\theta \cos\lambda \left(1 - \frac{a^5}{r^5}\right), \\ v_{0\theta} &= Ar \cos\lambda \left(-\sin^2\theta + \cos 2\theta \frac{a^5}{3r^5}\right), \\ v_{0\lambda} &= -\frac{Aa^5}{3r^4} \cos\theta \sin\lambda. \end{aligned}\right\} \tag{3.2}$$

Lighthill (1956*a*) has shown that $\boldsymbol{v}_1^{\mathrm{i}}$ is the Biot–Savart field of a system of vorticity within the sphere. Corresponding to an element of vorticity with strength

$$(\omega_{1r}, \omega_{1\theta}, \omega_{1\lambda})\, \mathrm{d}V$$

at the point (r, θ, λ) external to the sphere, there is an image system of vorticity with strength

$$\left(\frac{a}{r}\omega_{1r},\ -\frac{a}{r}\omega_{1\theta},\ -\frac{a}{r}\omega_{1\lambda}\right)\mathrm{d}V$$

at the image point $(a^2/r, \theta, \lambda)$ together with a uniform line vortex of strength

$$\left(-\frac{1}{a}\omega_{1r}, 0, 0\right)\mathrm{d}V$$

per unit length between the centre of the sphere and the image point. Rewriting this expression given in Lighthill (1956*a*) in terms of vectors, the Biot–Savart integral for $\boldsymbol{v}_1$ becomes

$$\boldsymbol{v}_1(\boldsymbol{r}) = \frac{1}{4\pi} \int \mathrm{d}r'\, \mathrm{d}\theta'\, \mathrm{d}\lambda'\, r'^2 \sin\theta'\, \boldsymbol{F}(\boldsymbol{r}, \boldsymbol{r}'), \tag{3.3}$$

where

$$\boldsymbol{F}(\boldsymbol{r},\boldsymbol{r}') = \frac{\boldsymbol{\omega}_1 \wedge (\boldsymbol{r}-\boldsymbol{r}')}{|\boldsymbol{r}-\boldsymbol{r}'|^3} - \left(\frac{a}{r'}\right)\frac{\overline{\boldsymbol{\omega}}_1 \wedge (\boldsymbol{r}-(a^2/r'^2)\boldsymbol{r}')}{|\boldsymbol{r}-(a^2/r^2)\boldsymbol{r}'|^3}$$
$$-\frac{1}{a}\left(\frac{\boldsymbol{\omega}_1 \cdot \boldsymbol{r}'}{r'^2}\right)\frac{\boldsymbol{r}' \wedge \boldsymbol{r}}{|\boldsymbol{r}-(\boldsymbol{r}\cdot\boldsymbol{r}'/r'^2)\boldsymbol{r}'|^2}\left\{\frac{\boldsymbol{r}\cdot\boldsymbol{r}'}{rr'} - \frac{(\boldsymbol{r}-(a^2/r'^2)\boldsymbol{r}')\cdot\boldsymbol{r}'}{|\boldsymbol{r}-(a^2/r'^2)\boldsymbol{r}'|\,r'}\right\} \quad (3.4)$$

and

$$\boldsymbol{\omega}_1 = \boldsymbol{\omega}_1(\boldsymbol{r}'),$$
$$\overline{\boldsymbol{\omega}}_1 = \boldsymbol{\omega}_1 - \frac{2(\boldsymbol{\omega}_1\cdot\boldsymbol{r}')\boldsymbol{r}'}{r'^2}.$$

4. Evaluation of $\boldsymbol{v}_1$

The main computational difficulty arises from the evaluation of the three-dimensional Biot–Savart integral (3.3) for $\boldsymbol{v}_1(\boldsymbol{r})$. The integrand has singularities at $\boldsymbol{r}' = \boldsymbol{r}$ and also as $r' \to a$, or $\theta' \to 0$, or $\theta' \to \pi$, where $(\partial t/\partial\rho_0)_\theta$, and consequently $\boldsymbol{\omega}_1$ is singular.

We shall require the values of $\boldsymbol{v}_1(\boldsymbol{r})$ on the surface of the sphere and also on the axis where $\theta = 0$ or π. Consequently, it is convenient to perform the integration with respect to ρ_0', rather than r', for when this is done, all the singularities are on the surface $\rho_0' = 0$. We rewrite the integral, then, in the form

$$\frac{1}{4\pi}\int_a^\infty \mathrm{d}r' \int_0^\pi \mathrm{d}\theta' \int_{-\pi}^{\pi} \mathrm{d}\lambda' r'^2 \sin\theta' \boldsymbol{F}(\boldsymbol{r},\boldsymbol{r}')$$
$$= \frac{1}{4\pi}\int_0^\infty \mathrm{d}\rho_0' \int_0^\pi \mathrm{d}\theta' \int_0^{2\pi} \mathrm{d}\lambda' r'^2 \sin\theta \left(\frac{\partial r'}{\partial \rho_0'}\right)_{\theta'} \boldsymbol{F}(\boldsymbol{r},\boldsymbol{r}'), \quad (4.1)$$

where

$$\boldsymbol{r}' = \boldsymbol{r}'(\rho_0', \theta')$$

is the positive solution of (2.16), and

$$\left(\frac{\partial r'}{\partial \rho_0'}\right)_{\theta'} = \frac{\rho_0' \operatorname{cosec}^2\theta'}{r'(1+a^3/2r'^3)}. \quad (4.2)$$

Thus, to determine $\boldsymbol{v}_1(\boldsymbol{r})$ at any point, one must perform a three-dimensional integration of the vector function $\boldsymbol{F}$. Some simplification is possible, however, using the axisymmetry of the system. When $r = a$ or when $\theta = 0$ or π

$$v_{1r} = 0;$$

when $\lambda = 0$ or π, we also have

$$v_{1\lambda} = 0$$

and when $\lambda = \frac{1}{2}\pi$ or $\frac{3}{2}\pi$

$$v_{1\theta} = 0.$$

$\boldsymbol{F}(\boldsymbol{r},\boldsymbol{r}')$ is a linear function of $\boldsymbol{\omega}_1(\boldsymbol{r}')$, so we can write it as

$$\boldsymbol{F}(\boldsymbol{r},\boldsymbol{r}') = \boldsymbol{\omega}_1(\boldsymbol{r}')\cdot\boldsymbol{G}(\boldsymbol{r},\boldsymbol{r}') \quad (4.3)$$

If $\boldsymbol{G}$ is written in terms of the local polar coordinate directions at the point $\boldsymbol{r}'$, then $\boldsymbol{G}$ depends upon λ and λ' only through the combination $\lambda - \lambda'$. As $\boldsymbol{\omega}_1(\boldsymbol{r}')$ can be written in the form

$$\omega_{1i}(\rho_0', \theta', \lambda') = \omega_{1i}(\rho_0', \theta', 0)\cos\lambda' + \omega_{1i}(\rho_0', \theta', \tfrac{1}{2}\pi)\sin\lambda' \quad (4.4)$$

where i stands for r', θ' or λ', it follows that

$$v_{1i}(r,\theta,\lambda) = v_{1i}(r,\theta,0)\cos\lambda + v_{1i}(r,\theta,\tfrac{1}{2}\pi)\sin\lambda. \quad (4.5)$$

This is a very useful result. Instead of integrating the vector $\boldsymbol{F}(\boldsymbol{r}, \boldsymbol{r}')$ over $\boldsymbol{r}'$ for each value of θ and λ where $\boldsymbol{v}_1(a, \theta, \lambda)$ is required, one only need integrate the scalar quantities $F_\theta(\boldsymbol{r}, \boldsymbol{r}')$ for each value of θ with $\lambda = 0$, and $\mathrm{F}_\lambda(\boldsymbol{r}, \boldsymbol{r}')$ for each value of θ with $\lambda = \frac{1}{2}\pi$ and use the following equations:

$$\left.\begin{aligned} &v_{1r}(r, \theta, \lambda) = 0 \quad \text{if } r = a \quad \text{or if } \theta = 0 \text{ or } \pi, \\ &v_{1\theta}(r, \theta, \lambda) = v_{1\theta}(r, \theta, 0) \cos\lambda, \\ &v_{1\lambda}(r, \theta, \lambda) = v_{1\lambda}(r, \theta, \tfrac{1}{2}\pi) \sin\lambda. \end{aligned}\right\} \tag{4.6}$$

This greatly reduces the effort required to calculate $\boldsymbol{v}_1$ over the surface of the sphere.

The numerical integrations cannot be performed satisfactorily by a standard numerical integration package because of the singularities of the integrand. Special techniques were developed for the integration and these will be described in the rest of this section. For definiteness we shall describe the calculation of $v_{1\theta}(a, \theta, 0)$. The calculation of $v_{1\lambda}(a, \theta, \frac{1}{2}\pi)$ and the velocity on the axis is very similar.

4.1. *The λ' integration*

The integration with respect to λ' is performed first. We denote the result of this integration by

$$F_1(\boldsymbol{r}, \rho_0', \theta') = \frac{1}{4\pi}\int_0^{2\pi} \mathrm{d}\lambda'\, r'^2 \sin\theta' \left(\frac{\partial r'}{\partial \rho_0'}\right) F_\theta(\boldsymbol{r}, r', \theta', \lambda'). \tag{4.7}$$

The integrand has a sharp peak near $\lambda' = \lambda$ when ρ_0 is small. To handle this integration efficiently and accurately we use a change of variable from λ' to ζ, where

$$\tan(\tfrac{1}{2}\lambda') = c^{\frac{1}{2}} \tan(\tfrac{1}{2}\zeta) \tag{4.8}$$

with

$$c = \frac{r^2 + r'^2 - 2rr'\cos(\theta + \theta')}{r^2 + r'^2 - 2rr'\cos(\theta - \theta')}, \tag{4.9}$$

and integrate using an adaptive routine from the NAG library (D01AJF), which is designed to integrate functions with singularities, or near-singular behaviour. The calculations were performed with a requested relative error tolerance of 10^{-4}. Generally the accuracy attained was better than this, but for a few values of ρ_0' and θ' this accuracy could not be attained due to rounding error; however, in these cases the absolute value of the integral is small and makes a negligible contribution to the secondary velocity.

4.2. *The θ' integration*

When ρ_0' is small it is found that $F_1(\boldsymbol{r}, \rho_0', \theta')$ has a sharp spike around the value of θ' at which

$$s^2 = r^2 + r'^2 - 2rr'\cos(\theta - \theta') \tag{4.10}$$

is minimized with $r' = r'(\rho_0', \theta')$. The spikiness of the integrand may be substantially reduced by the following change of variable:

$$\xi = \xi_0 - \alpha \operatorname{arcsinh}\left(\frac{\theta' - \hat{\theta}}{\delta}\right), \tag{4.11}$$

where $\hat{\theta}$ and δ are chosen such that

$$s^2 \sim s_{\min}^2 \left(1 + \frac{(\theta' - \hat{\theta})^2}{\delta^2}\right) \quad \text{as } \theta' - \hat{\theta} \to 0, \tag{4.12}$$

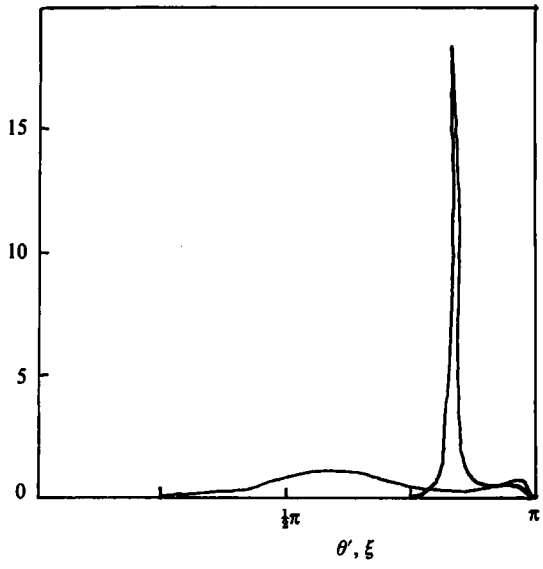

FIGURE 2. The smoothing of the θ' integrand $F_1(r, \rho_0', \theta')$ caused by change of variable from θ' to ξ, (4.13), $r = a$, $\theta = 5\pi/6$, $\lambda = 0$, $\rho_0' = 0.113$.

and α and ξ_0 are chosen such that

$$\xi = 0 \quad \text{when } \theta' = 0,$$

and

$$\xi = \pi \quad \text{when } \theta' = \pi.$$

With this change of variable the integral is transformed to

$$\int_0^\pi \mathrm{d}\theta' \, F_1(r, \rho_0', \theta) = \frac{\delta}{\alpha} \int_0^\pi \mathrm{d}\xi \, F_1(r, \rho_0', \theta'(\xi)) \cosh\left(\frac{\xi - \xi_0}{\alpha}\right). \tag{4.13}$$

Notice that $\cosh(\xi - \xi_0/\alpha)$ has a minimum at the place where $F_1(r, \rho_0', \theta')$ has a peak. The smoothing effect of this change is shown in figure 2.

The integration was performed using the same software as the λ' integration, and the same error tolerance, 10^{-4}. (To be exact, a copy of the routine with different subroutine and variable names was used, as Fortran is not a recursive language.)

We shall denote the result of the θ' integration by $F_2(r, \rho_0')$.

4.3. *The ρ_0' integration*

The most obvious difficulty in the ρ_0' integration is that the range of integration is infinite. A further complication arises at the stagnation points, where $r = a$, $\theta = 0$ or π, as $F_2(r, \rho_0')$ becomes infinitely large as ρ_0' tends to zero. These difficulties are handled using a Gauss-Rational quadrature scheme, using the NAG routine D01BCF to evaluate the weights and abscissae. The scheme is exact for integrals of the form

$$\int_0^\infty \frac{x^c}{(1+x)^d} P_n\left(\frac{1}{1+x}\right) \mathrm{d}x, \tag{4.14}$$

where

$$a > 0, \quad d - 1 > c > 1$$

and P_n is a polynomial of order $2n-1$ or less, n being the number of evaluation points.

The values of a, c and d are chosen by the user on the basis of his knowledge of

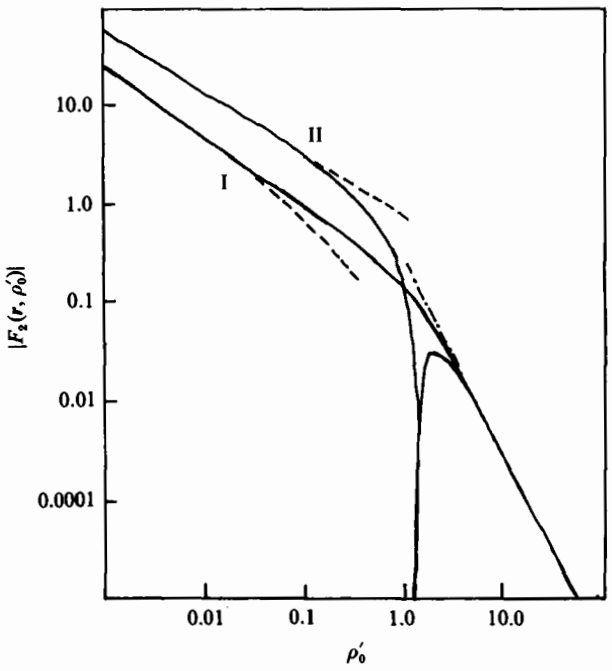

FIGURE 3. Logarithmic graph of integrand of the ρ_0' integration $F_2(r,\rho_0')$ when r is, (I), the front and, (II), the rear stagnation point on the sphere. Notice the singular behaviour as $\rho_0' \to 0$. The dashed curves are the asymptotic approximations (4.17) and (4.18) and the dot-dashed curve is (4.19).

the integrand. Except at the stagnation points the asymptotic behaviour of $F_2(r,\rho_0')$ for small and large ρ_0' is

$$\frac{F_2(r,\rho_0')}{A} = \begin{cases} O(1) & \text{as } \dfrac{\rho_0'}{a} \to 0, \\ O\left(\dfrac{\rho_0'}{a}\right)^{-2} & \text{as } \dfrac{\rho_0'}{a} \to \infty, \end{cases} \tag{4.15}$$

and the chosen values of a, c and d are 1, 0 and 2 respectively. At the stagnation points the behaviour of F_2 is singular as $\rho_0' \to 0$ and the numerical values plotted in figure 3 suggest that

$$\frac{F_2(r,\rho_0')}{A} = \begin{cases} O\left(\dfrac{\rho_0'}{a}\right)^{-\frac{2}{3}} & \text{as } \dfrac{\rho_0'}{a} \to 0, \\ O\left(\dfrac{\rho_0'}{a}\right)^{-2} & \text{as } \dfrac{\rho_0'}{a} \to \infty, \end{cases} \tag{4.16}$$

and corresponding values of c and d are $-\frac{2}{3}$ and $\frac{4}{3}$ respectively. The asymptotic behaviour of $F_2(r,\rho_0')$ for small ρ_0' can also be obtained from the integral expressions given by Lighthill (1957, equation (10.13)). The dominant contribution to F_2 comes from the vorticity at points very close to r and detailed analysis, not given here, shows that

$$\frac{F_2(r,\rho_0')}{A} \sim C\left(\left(\frac{\rho_0'}{a}\right)^{-\frac{2}{3}} - \left(\frac{\rho_0'}{a}\right)^{-\frac{1}{3}} + O(1)\right) \tag{4.17}$$

at the front stagnation point $r = a$, $\theta = \pi$, and

$$\frac{F_2(r,\rho_0')}{A} \sim C\left(-2\left(\frac{\rho_0'}{a}\right)^{-\frac{2}{3}} - \left(\frac{\rho_0'}{a}\right)^{-\frac{1}{3}} + O(1)\right) \tag{4.18}$$

θ	$\frac{v_\theta(a,\theta,0)}{Aa}$	$\frac{v_\lambda(a,\theta,\frac{1}{2}\pi)}{Aa}$
0	−1.1803	1.1803
10	−0.2284	0.5343
20	0.0255	0.3118
30	0.0706	0.1917
40	−0.0152	0.1393
50	−0.1734	0.1376
60	−0.3525	0.1747
70	−0.5079	0.2416
80	−0.6050	0.3302
90	−0.6207	0.4335
100	−0.5451	0.5448
110	−0.3817	0.6583
120	−0.1461	0.7685
130	0.1361	0.8705
140	0.4331	0.9601
150	0.7104	1.0337
160	0.9357	1.0883
170	1.0824	1.1220
180	1.1327	1.1327

$$v_\theta(a,\theta,\lambda) = v_\theta(a,\theta,0)\cos\lambda$$
$$v_\lambda(a,\theta,\lambda) = v_\lambda(a,\theta,\tfrac{1}{2}\pi)\sin\lambda$$

TABLE 5. Secondary velocity on sphere surface

r/a	$\frac{v_\theta(r,\pi,0)}{Aa}$
1.0000	1.1327
1.0196	0.9469
1.0824	0.7383
1.2027	0.5185
1.4142	0.3221
1.8000	0.1704
2.6131	0.07032
5.1258	0.01650

$$v_r(r,\pi,0) = 0$$
$$v_\lambda(r,\pi,0) = 0$$

TABLE 6. Secondary velocity on upstream axis

at the rear stagnation point, $r = a$, $\theta = 0$. The constant C is given by

$$C = 3^{-\frac{1}{3}}B(\tfrac{2}{3},\tfrac{5}{6}) \sim 0.2764,$$

where B is a beta function (Abramowitz & Stegun 1965, p. 258). The behaviour as $\rho_0' \to \infty$ can also be determined, and

$$\frac{F_2(r,\rho_0')}{A} \sim \frac{5\pi}{64\rho_0'^2} \tag{4.19}$$

for both the stagnation points. A contribution $\pi/64\rho_0'^2$ comes from the θ-vorticity as stated by Lighthill (1957, equation 21) and the remaining $4\pi/64\rho_0'^2$ from the

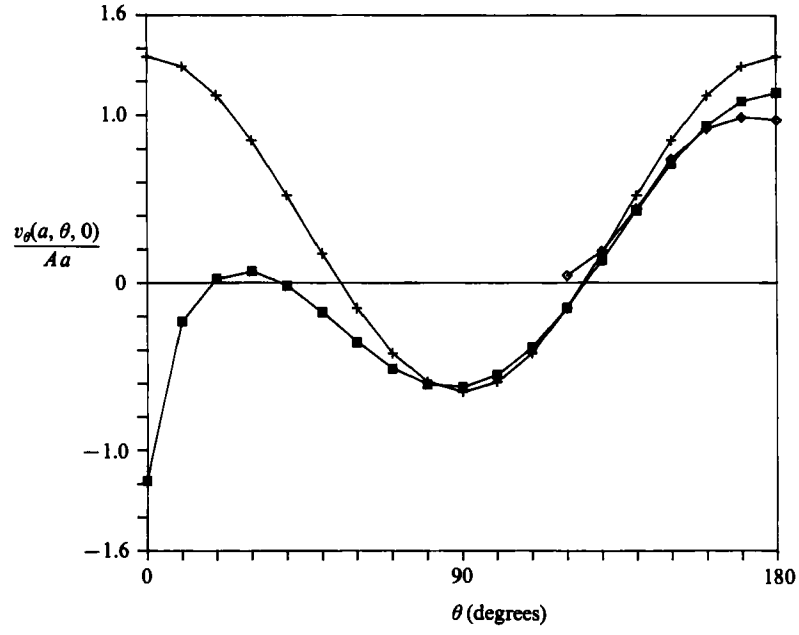

FIGURE 4. Secondary θ-velocities on the surface of the sphere in the plane of symmetry: $v_\theta(a,\theta,0)/Aa$: ■, the numerical results of this paper, ◇, Cousins (1969) numerical results, and the curve + is Hall's (1956) approximate analytical results.

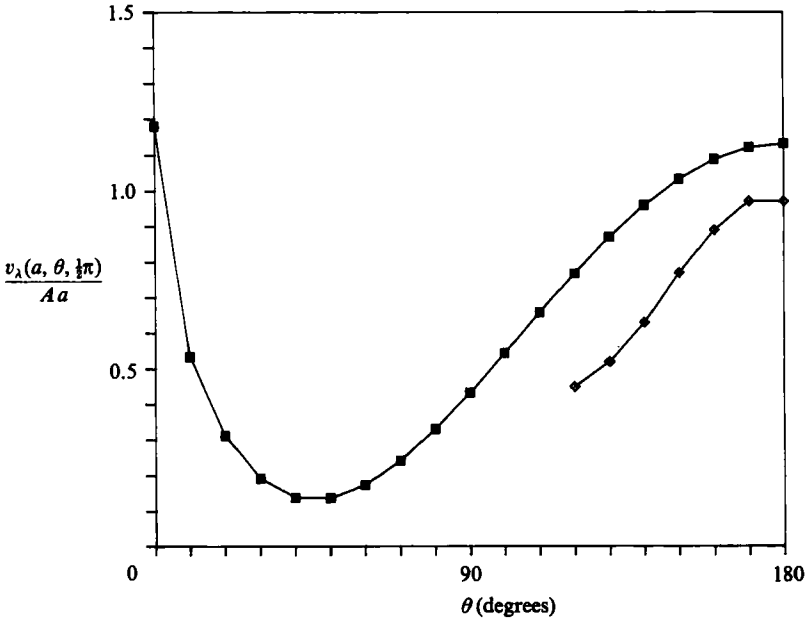

FIGURE 5. Secondary λ-velocities on the surface of the sphere: $v_\lambda(a,\theta,\frac{1}{2}\pi)/Aa$: ■, the numerical results of this paper; ◇, those of Cousins (1969).

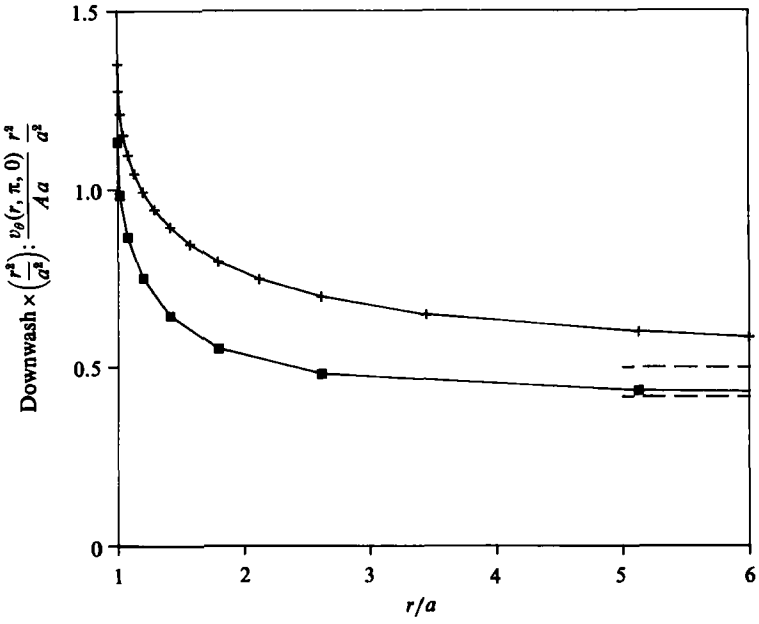

FIGURE 6. Downwash on upstream axis times r^2/a^2: $(v_\theta(r,\pi,0)/Aa)$ (r^2/a^2): ■, numerical results of this paper; +, Hall's (1956) approximation, and the dashed lines are the asymptotic limits of the two graphs.

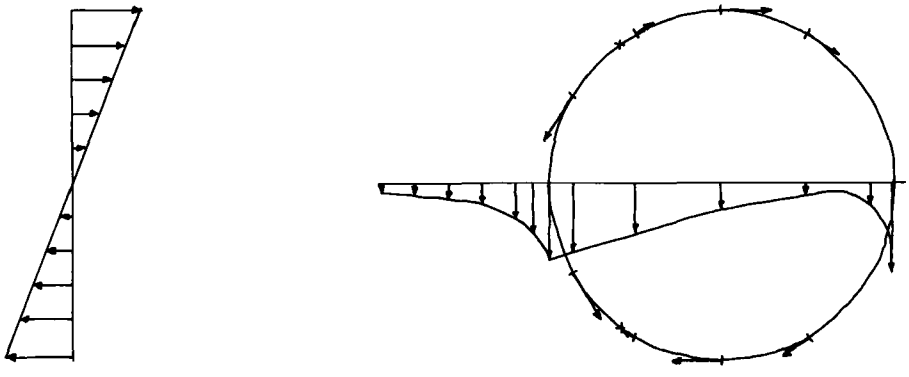

FIGURE 7. Diagram showing directions and magnitudes of secondary velocities in the oncoming shear flow and on the sphere surface.

λ-vorticity. These asymptotic formulae are also plotted on figure 3 and the close agreement between the asymptotic and numerical results provides an independent check upon the calculation.

The ρ_0' integrations were performed with 32, or in some cases 64, points of evaluation.

The calculated values of v_θ and v_λ (including v_0) on the surface of the sphere, and the downwash, v_θ on the upstream axis are given in tables 5 and 6. As stated above, the λ' and θ' integrations are accurate to at least four significant figures. Halving the number of integration points used for the ρ_0' integration gives results that differ from those of tables 5 and 6 by less than 10^{-5}. The values given in the tables are believed to be accurate to at least three significant figures.

These results are plotted on figures 4, 5 and 6. To give a clearer picture, the magnitude and direction of the secondary velocity at certain points on the sphere surface and on the upstream axis is shown on figure 7.

5. The lift force on the sphere

By Bernoulli's theorem, neglecting gravity,

$$h = p + \tfrac{1}{2}\rho|u|^2$$

is constant along the streamlines. Therefore, on the surface of the sphere the pressure is

$$p = p_0 + \tfrac{1}{2}\rho|u_0|^2 - \tfrac{1}{2}\rho|\boldsymbol{u}|^2, \tag{5.1}$$

where p_0 and u_0 are the pressure and velocity far upstream on the stagnation streamline.

To first order in the oncoming vorticity, A,

$$\tfrac{1}{2}|\boldsymbol{u}|^2 = \tfrac{1}{2}V_\theta^2 + V_\theta v_\theta + O(A^2a^2), \tag{5.2}$$

and the lift force on sphere is therefore

$$\begin{aligned}\boldsymbol{F}_L &= \int_S -p\boldsymbol{n}\,\mathrm{d}S \\ &= \rho\int_0^\pi \mathrm{d}\theta \int_0^{2\pi} \mathrm{d}\lambda\, a^2 \sin\theta \tfrac{3}{2}u_0 \sin\theta\, v_\theta(a,\theta,0)\cos\lambda\boldsymbol{n},\end{aligned} \tag{5.3}$$

where S is the surface of sphere and (4.6) has been used for $v_\theta(a,\theta,\lambda)$.

In Cartesian coordinates

$$\boldsymbol{n} = \begin{pmatrix} \cos\theta \\ \sin\theta\cos\lambda \\ \sin\theta\sin\lambda \end{pmatrix}.$$

By inspection F_y is the only non-zero component of $\boldsymbol{F}_L$ and

$$\begin{aligned}F_y &= \frac{3\pi}{2}\rho^* a^2 u_0 \int_0^\pi \mathrm{d}\theta \sin^3\theta\, v_\theta(a,\theta,0) \\ &\approx 2.09454\rho^* a^3 u_0 A,\end{aligned} \tag{5.4}$$

and in vector notation

$$\left.\begin{aligned}\boldsymbol{F}_L &= C_L \rho^* \tfrac{4}{3}\pi a^3 \boldsymbol{u}_0 \wedge \boldsymbol{\omega}_0, \\ C_L &\approx 0.500035.\end{aligned}\right\} \tag{5.5}$$

This result is obtained by numerical integration using Simpson's rule and the values of v_θ given in table 5.

This result is used in developing a general expression for the lift force and the total force acting on a small sphere in an arbitrary rotational straining flow, by Auton *et al.* (1987).

6. An analytical evaluation of the lift coefficient

The reader will have noticed that the computed value of the lift coefficient is remarkably close to $\frac{1}{2}$. In this section we present an analytical argument to prove that the value is exactly $\frac{1}{2}$.

Applying the momentum-integral theorem to a volume surrounding the sphere we find that

$$-\boldsymbol{F}_L = \int_S \{\rho^*(\boldsymbol{u}\cdot\boldsymbol{n})\,\boldsymbol{u} + p\boldsymbol{n}\}\,\mathrm{d}S, \tag{6.1}$$

where S is the external surface of the volume of integration. It is convenient to choose for S a deformed cylinder, whose curved surface is parallel to the streamlines of the primary flow, and bounded axially by circular disks of radius Σ centred on the x-axis at positions $x = \pm X$ (see figure 8). Σ and X are chosen such that

$$a \ll \Sigma \ll \frac{U}{A}, \tag{6.2}$$

$$X \gg \Sigma. \tag{6.3}$$

Using Bernoulli's theorem we can expand p in terms of the velocity

$$p = p_0 + \tfrac{1}{2}\rho^*(\boldsymbol{u}^{-\infty})^2 - \tfrac{1}{2}\rho^*(\boldsymbol{u})^2, \tag{6.4}$$

where $\boldsymbol{u}^{-\infty}$ is the velocity far upstream on the same streamline and p_0 is the uniform upstream pressure. The total velocity is made up of the irrotational primary flow $\boldsymbol{V}$, proportional to $\boldsymbol{u}$, and a secondary velocity $\boldsymbol{v}$, proportional to A. The terms involving only $\boldsymbol{V}$ contribute nothing to the total integral as there is no net force due to a uniform streaming motion, the interaction of $\boldsymbol{V}$ and $\boldsymbol{v}$ leads to a force in the y-direction, which is proportional to A. In the following analysis we shall consider only those terms that are first order in A and only the y-component of the force integral.

Consider now the far field of $\boldsymbol{v}$. In the wake, far downstream of the sphere, the vorticity is aligned in the x-direction, with

$$\omega_x = A \sin\lambda \frac{\mathrm{d}X}{\mathrm{d}\rho} \tag{6.4}$$

(Lighthill 1956*b*) where

$$X = \lim_{x\to\infty} u_0 t(x,\rho). \tag{6.5}$$

This vorticity induces a flow in the (y,z)-plane, given by

$$\left.\begin{aligned} v_y &= -A\cos 2\lambda \frac{1}{\rho^2}\int_0^\rho \rho'\,\mathrm{d}\rho'\,X(\rho') - \tfrac{1}{2}(1-\cos 2\lambda)\,X(\rho) \\ v_z &= -A\sin 2\lambda \frac{1}{\rho^2}\int_0^\rho \rho'\,\mathrm{d}\rho'\,X(\rho') + \tfrac{1}{2}\sin 2\lambda X(\rho), \end{aligned}\right\} \tag{6.6}$$

independent of x. Outside the wake region, the secondary flow far from the sphere is given by

$$\boldsymbol{v} \sim A\rho\cos\lambda\boldsymbol{e}_x + \frac{Aa^3}{2r^3}(-\rho\cos\lambda, x, 0) + \frac{Aa^3}{6}\nabla\left(\frac{\cos\lambda}{\rho}\left(1+\frac{x}{r}\right)\right) \tag{6.7}$$

(Lighthill 1956*b*). We can now evaluate the leading-order terms in the force integral.

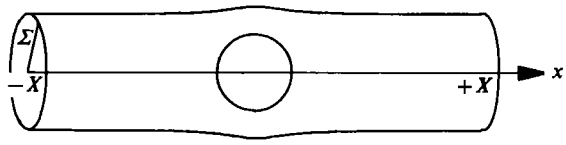

FIGURE 8. Sketch showing volume of integration used in the analysis of §6.

On the upstream disk all terms of the integral vanish asymptotically, as $x/a \to \infty$. On the curved surface S_1 the leading-order term is

$$\rho^* \int_{S_1} -n_y(\boldsymbol{v}-\boldsymbol{v}^{-\infty})\cdot\boldsymbol{V}^{-\infty}\,\mathrm{d}S, \tag{6.8}$$

where
$$\boldsymbol{V}^{-\infty} = u_0 \boldsymbol{e}_x \tag{6.9}$$

and
$$\boldsymbol{v}^{-\infty} = A\rho^{-\infty}\boldsymbol{e}_x \cos\lambda \tag{6.10}$$

are the asymptotic limits of $\boldsymbol{V}$ and $\boldsymbol{v}$, and $\rho^{-\infty}$ of ρ, as $x \to -\infty$ along a streamline.

To leading order, from (6.7) and (6.10)

$$(\boldsymbol{v}-\boldsymbol{v}^{-\infty})_x \sim \frac{A\rho a^3 \cos\lambda}{6r^3} \tag{6.11}$$

as
$$\rho - \rho^{-\infty} \sim \frac{a^3}{2r^3}\rho. \tag{6.12}$$

To leading order we can approximate ρ by Σ, and the integral becomes

$$\rho^* \int_{-x}^{x} \mathrm{d}x \int_0^{2\pi} \Sigma\,\mathrm{d}\lambda(-\cos\lambda)\frac{Aa^3\Sigma\cos\lambda u_0}{6(\Sigma^2+x^2)^{\frac{3}{2}}} \sim -\tfrac{1}{3}\pi a^3\rho^* A u_0\left(1+O\left(\frac{\Sigma^2}{X^2}\right)\right). \tag{6.13}$$

On the downstream disk S_2 the leading-order term is

$$\rho^* \int_{S_2} (\boldsymbol{n}\cdot\boldsymbol{V})\, v_y\,\mathrm{d}S, \tag{6.14}$$

and substituting for v_y, its asymptotic form in the far downstream wake region (6.6), this becomes

$$\rho^* \int_0^{\Sigma} \rho\,\mathrm{d}\rho \int_0^{2\pi} \mathrm{d}\lambda\, u_0\left(-\frac{A\cos 2\lambda}{\rho^2}\int_0^{\rho}\rho'\,\mathrm{d}\rho' X(\rho') - \tfrac{1}{2}A(1-\cos 2\lambda)\,X(\rho)\right)$$

$$\sim -\tfrac{1}{2}u_0 A\rho^* \int_{0_1}^{\infty} \rho\,\mathrm{d}\rho\, X(\rho) = -\tfrac{1}{2}u_0 A\rho^* V_n = -\tfrac{1}{3}\pi a^3\rho^* u_0 A, \tag{6.15}$$

where $V_n = \frac{1}{2}V$ is the drift volume associated with the primary flow (Darwin 1953).

Putting the separate contributions together, we conclude that

$$\boldsymbol{F}_L = -\tfrac{2}{3}\pi a^3\rho^* u_0 A \boldsymbol{e}_y \tag{6.16}$$

and
$$C_L = \tfrac{1}{2}. \tag{6.17}$$

7. Discussion

In this paper Lighthill's secondary-flow method is used to expose features of the flow around a stationary sphere placed in a simple shear flow. The secondary flow on the sphere surface has been calculated numerically, and used to estimate the resulting lift force on the sphere.

Lighthill's work is mainly concerned with calculating the secondary velocity on the upstream axis, which he calls the downwash, $D(r)$, and the displacement of the stagnation streamline δ; δ is used to correct the results of Pitot-tube velocity measurements from sheared velocity fields. In our notation

$$D(r) = v_\theta(r, \pi, 0). \tag{7.1}$$

Wherever possible, the results of this paper have been compared with Lighthill's and this has provided a check upon the analysis. This comparison has shown a couple of minor errors in Lighthill (1957, hereinafter denoted L).

In the final, ρ_0', integration for $D(r)$, Lighthill claims that the integrand $D_\theta(r, \rho_0')$ tends to zero as $\rho_0' \to 0$ (L, p. 500). (The suffix θ here denotes the Biot–Savart contribution to $D(r)$ from $\omega_{1\theta}$ – he obtains the contribution from $\omega_{1\lambda}$ analytically and $D_r(r, \rho_0') \to 0$ as claimed.) This is only true, however, when $r > a$; at $r = a$ careful asymptotic analysis of the expression given by Lighthill (L, equation 13) shows that

$$D(a, \rho_0') \sim C\rho_0'^{-\frac{1}{3}} \quad \text{as } \rho_0' \to 0. \tag{7.2}$$

This result is confirmed by the numerical results shown in figure 3. Consequently Lighthill's value for $D(a)$ of $0.97Aa$ is too small by 15% compared with our result of $1.133Aa$. At larger values of r Lighthill's results are confirmed: he gives

$$D(\sqrt{2}a) = 0.33Aa, \tag{7.3}$$

compared with $0.322Aa$ found in this paper, and Lighthill's asymptotic result (L, equation (22))

$$D(r) \sim \frac{5}{12}\left(\frac{a}{r}\right)^2 Aa \tag{7.4}$$

is also confirmed by our numerical results.

The displacement of the stagnation streamline is given by (L, equations (31), (32))

$$\delta = \frac{1}{u_0}\int_a^\infty \frac{D(r)\,\mathrm{d}r}{(1-a^3/r^3)^{\frac{1}{3}}} = \frac{1}{u_0}\int_0^{\frac{1}{2}\pi} \frac{D(a\,\mathrm{cosec}\,\alpha)}{(1-\sin^3\alpha)^{\frac{1}{3}}}\,\mathrm{cosec}\,\alpha\,\cot\alpha\,\mathrm{d}\alpha, \tag{7.5}$$

where $\alpha = \arcsin a/r$. Lighthill estimates δ using Simpson's rule, with interval $\frac{1}{4}\pi$ and the second integral above, and finds

$$\delta \approx \frac{Aa^2}{u_0}\frac{\pi}{12}\{\tfrac{5}{12} + 7.036D(\sqrt{2}a) + \tfrac{2}{3}D(a)\}. \tag{7.6}$$

However, the coefficient of $D(a)$ should be $\frac{2}{3}\frac{1}{2}$ here and Lighthill's estimate of $D(a)$ is itself too small. The effect upon δ is quite small, though, and Lighthill's value of $0.89Aa^2/u_0$ is quite close to our estimate, based upon the figures in table 6, of $0.938Aa^3/u_0$; his value of δ is accurate to one decimal place, despite these errors, which is all the accuracy he claims.

A similar calculation to that given here has also been made by Cousins (1969, 1970). He used Lighthill's theory to calculate numerically the secondary velocities over a portion of the forward surface of the sphere, where $\theta > 120°$. He claims an accuracy of one decimal place in his values of v but makes no mention of any special procedures being used because of singularities of the Biot–Savart integrand. The accuracy of his results must be questioned as he obtains the same, erroneous, value as Lighthill, $0.97Aa$, for the downwash at the front stagnation point. He does not appear to have noticed the trigonometric relations (4.6), which would have

substantially reduced his computational labours. In terms of Cartesian coordinates, as used by Cousins, the relations (4.6) imply

$$\left.\begin{aligned} v_x(r,\theta,\lambda) &= v_x(r,\theta,0)\cos\lambda, \\ v_y(r,\theta,\lambda) &= v_y(r,\theta,0)\cos^2\lambda + v_y(r,\theta,\tfrac{1}{2}\pi)\sin^2\lambda, \\ v_z(r,\theta,\lambda) &= v_z(r,\theta,\tfrac{1}{4}\pi)\sin 2\lambda. \end{aligned}\right\} \tag{7.7}$$

Alternatively, these relations can be derived quite easily from the expressions given in Appendix I of Cousins' (1969) paper, but they are not satisfied by Cousins' results, even allowing an error of ± 0.1 on each figure. For comparison some of his results are plotted on figures 4 and 5.

Hall (1956) has found an approximation to the secondary velocity in the plane of symmetry. He assumes that the two-dimensional divergence of v in this plane is zero so that

$$\frac{\partial v_x}{\partial x} + \frac{\partial v_y}{\partial y} = 0. \tag{7.8}$$

This is only an approximation, as $\partial v_z/\partial z \neq 0$ in general. The curl of the velocity in this plane is

$$\frac{\partial v_y}{\partial x} - \frac{\partial v_x}{\partial y} = \omega_z \tag{7.9}$$

with ω_z the same as that used in this paper,

$$\omega_z = \frac{-A}{(1-a^3/r^3)}. \tag{7.10}$$

With this approximation an analytic solution in the plane of symmetry can be found, viz.

$$\left.\begin{aligned} \frac{v_r}{Aa} &= \frac{1}{2}\left(\frac{r}{a} - \frac{a^3}{r^3}\right)\sin 2\theta \\ \frac{v_\theta}{Aa} &= -\frac{1}{2}\frac{r}{a} + \frac{a}{r}\int_{r/a}^{\infty} (x^{\frac{5}{2}}(x^3-1)^{-\frac{1}{2}} - x)\,\mathrm{d}x + \frac{1}{2}\left(\frac{r}{a} + \frac{a^3}{r^3}\right)\cos 2\theta. \end{aligned}\right\} \tag{7.11}$$

For comparison with our results these velocities are also plotted on figures 4 and 6. Hall's method generally overestimates the downwash and, hence the displacement δ. Using Hall's theory one finds

$$\frac{u_0\,\delta}{Aa^2} \approx 1.24 \tag{7.12}$$

which is 30 % larger than our result. On the surface of the sphere, Hall's values of v_θ are surprisingly close to ours for $\theta > \frac{1}{2}\pi$, but on the downstream face of the sphere, the other vorticity components, ω_r and ω_θ, neglected in Hall's theory, become more significant and the results diverge. The lift coefficient, estimated using Hall's values for v_θ, is 0.375 and is about 30 % smaller than the result of this paper.

The numerical value for the lift coefficient is confirmed by a more elegant analytical argument, using the momentum theorem. It is instructive to reiterate the assumptions underlying this analysis. The momentum theorem is applied to a control volume surrounding the sphere, which is a slightly deformed cylinder, the generators being streamlines of the primary flow. An approximation to the momentum integral is then found, using far-field results for the secondary flow, published by Lighthill 1956*b*, in the case that the cylinder diameter is much larger than the sphere diameter, and

its length much greater than its diameter. However, as Lighthill (1957) has pointed out the approximations to the far-field secondary velocity are only valid when

$$a \ll r \ll a/\tilde{A}.$$

The expression for the lift force is thus found as an approximation to a momentum integral over a finite volume, and should be viewed as the first term in an asymptotic expansion in $\tilde{A}$.

To obtain this result, it is necessary to assume that the cylinder is much longer than its diameter. This is analogous to Darwin's (1953) observation that, to calculate the drift volume of the sphere moving through an infinite fluid at rest, it is necessary to take limits in the x-direction and in the ρ-direction, in that order. This same point has recently been reiterated by Benjamin (1986). It is interesting to note, however that the integral for $\boldsymbol{F}_L$ has leading-order contributions from the curved surface S_1 and from the downstream disk S_2, whilst the drift volume has contributions only from the upstream and downstream disks.

In a later paper (Auton *et al.* 1987) it will be shown how the result found here for $\boldsymbol{F}_L$ may be generalized to more complex, straining and time-dependent inviscid flows.

In a real fluid, viscosity will act to cause a drag force opposing the relative motion of the fluid, and may cause separation of the flow from the rear of the sphere. The effect of flow separation is difficult to determine, but is likely to be less significant for bodies with mobile surfaces, such as bubbles and drops, than for rigid particles.

The effects of finite drag on the motion of bubbles is discussed in Thomas *et al.* (1983), and some of the experimental data on the forces on spherical bodies is reviewed in Auton (1984).

This work was supported by the Science and Engineering Research Council and the Central Electricity Research Laboratory under a CASE studentship. I wish to acknowledge my debt of gratitude to my Ph.D. supervisors, Dr J. C. R. Hunt and Dr N. H. Thomas, for much helpful guidance and encouragement and to the referees of earlier drafts of this paper for their comments.

REFERENCES

Abramowitz, M. & Stegun, I. A. 1965 *Handbook of Mathematical Functions*. National Bureau of Standards.

Auton, T. R. 1984 The dynamics of bubbles drops and particles in motion in liquids. Ph.D. thesis, University of Cambridge.

Auton, T. R., Hunt, J. C. R. & Prud'homme, M. 1987 On the motion of a circular cylinder and a sphere in inviscid rotational flow. *J. Fluid Mech.* (submitted).

Batchelor, G. K. 1967 *An Introduction to Fluid Dynamics*. Cambridge University Press.

Benjamin, T. B. 1986 Note on added mass and drift. *J. Fluid Mech.* **169**, 251.

Cousins, R. R. 1969 Shear flow past a sphere. *NPL rep.* MA80.

Cousins, R. R. 1970 A note on the shear flow past a sphere. *J. Fluid Mech.* **40**, 543.

Darwin, C. 1953 Note on hydrodynamics. *Proc. Camb. Phil. Soc.* **49**, 342.

Hall, I. M. 1956 The displacement effect of a sphere in a two-dimensional flow. *J. Fluid Mech.* **1**, 142.

Lighthill, M. J. 1956*a* The image system of a vortex element in a rigid sphere. *Proc. Camb. Phil. Soc.* **52**, 31.

Lighthill, M. J. 1956*b* Drift. *J. Fluid Mech.* **1**, 31 (and Corrigendum **2**, 311).

Lighthill, M. J. 1957 Contributions to the theory of the Pitot tube displacement effect. *J. Fluid Mech.* **2**, 493.

TAYLOR, G. I. 1928 The forces on a body placed in a curved or converging stream of fluid. *Proc. R. Soc. Lond.* A **70**, 260.

THOMAS, N. H., AUTON, T. R., SENE, K. J. & HUNT, J. C. R. 1983 Entrapment and transport of bubbles by transient large eddies in multiphase turbulent shear flows. *BHRA Intl Conf. on the Physical Modelling of Multiphase flows, Coventry, April 1983* , p. 169. (Also 1984 Entrapment and transport of bubbles by plunging water. In *Gas Transfer at Water Surfaces* [ed. W. Brutsaert & G. H. Jirka], p. 255. Reidel.)

TOLLMIEN, W. 1938 Uber Krafte und Momente in schwach gekrummten oder konvergenten Stromungen. *Ing.-Arch.* **9**, 308.